

Bifunctional Photocatalysts Display Proximity-Enhanced Catalytic Activity in Metallaphotoredox C–O Coupling

Luigi Dolcini, Andrea Solida, Daniele Lavelli, Andrés Mauricio Hidalgo-Núñez, Tommaso Gandini, Matthieu Fornara, Alessandro Colella, Alberto Bossi, Marta Penconi,* Daniele Fiorito, Cesare Gennari, Alberto Dal Corso, and Luca Pignataro*



Cite This: *ACS Catal.* 2024, 14, 18651–18659



Read Online

ACCESS |



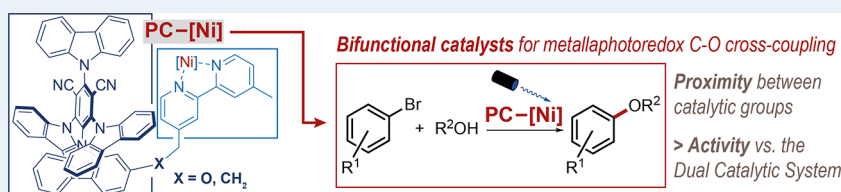
Metrics & More



Article Recommendations



Supporting Information



ABSTRACT: Dual catalytic reactions may be made more effective through improved integration of the catalytic cycles achieved using bifunctional catalysts. Herein, we describe two bifunctional photocatalysts consisting of a photoactive donor–acceptor cyanoarene unit linked to a bipyridine ligand moiety that can bind transition metals. The bifunctional photocatalysts were synthesized in 3–5 steps from commercially available compounds and fully characterized in terms of photophysical properties, which are strongly affected by the type of linkage used (C vs O) to connect the cyanoarene core to the ligand. Catalytic tests carried out in the Ni-catalyzed C–O cross-coupling of alcohols to aryl bromides promoted by visible light have shown that the bifunctional systems are more active than the corresponding “dual catalytic systems” (i.e., not covalently bound), taking advantage of the proximity between the two catalytic moieties (Ni-complex and photocatalyst). The best bifunctional photocatalysts were tested with several alcohols and aryl halides, giving good yields at low catalytic loading (0.5–2 mol %).

KEYWORDS: metallaphotoredox catalysis, bifunctional catalysis, donor–acceptor cyanoarenes, cross-coupling, visible light

INTRODUCTION

The bifunctional approach to catalysis has been exploited in many instances to achieve improved yield, selectivity, or even novel types of reactivity. Owing to proximity, two (or more) covalently linked functional groups may operate synergistically and combine different types of activation more effectively than the corresponding “dual systems” (i.e., employing two distinct catalysts). This benefit also brings along an intrinsic limitation in terms of flexibility, as independent variation of the two catalytic moieties and their stoichiometric ratio is not possible anymore. Bifunctionality is best represented in organocatalysis, with some archetypical catalysts (e.g., proline) being bifunctional, as well as many others developed by rational design.¹ Moreover, several bifunctional transition metal catalysts have been reported: besides the ligand necessary to bind the metal, these systems possess an additional functional group capable of substrate binding/activation and (or) formation of “supramolecular bidentate ligands”.² In the context of blossoming interest for visible light photocatalysis observed in the last two decades, several bifunctional photocatalysts have been reported.³ Indeed, many visible light-promoted transformations are actually dual catalytic reactions⁴ and thus hold an evident potential for a bifunctional approach. So far, most efforts have been devoted to enantioselective catalysts, and

photocatalysts have been linked to several types of chiral catalysts such as amines,⁵ lactams,⁶ thioureas,⁷ Brønsted acids,⁸ cinchona-derived ammonium salts,⁹ and Ni-BOX complexes.¹⁰ Although transition metal photocatalysts have been also employed,^{5b,6b,c} most bifunctional photocatalysts rely on organic dyes, with thioxanthone taking the lion’s share. We envisioned that the bifunctional approach, besides the enantioselectivity issue, could generally enhance the performance of dual catalytic reactions by ensuring better integration between the relevant catalytic cycles. In the context of bifunctional metallaphotoredox catalysis, Song and Lee recently demonstrated this approach with artificial photocatalytic enzymes possessing both an Ir-photocatalyst and a Ni(bpy) complex, which effectively catalyze the visible light-promoted synthesis of phenols from aryl halides.¹¹

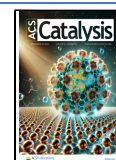
Herein, we describe structurally simpler bifunctional systems featuring an organic photocatalyst connected to a 2,2’-

Received: September 25, 2024

Revised: November 26, 2024

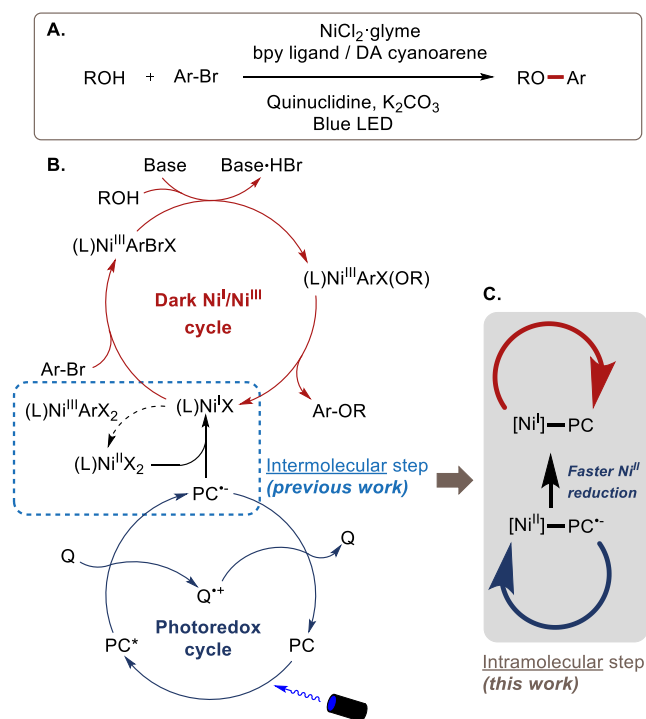
Accepted: November 26, 2024

Published: December 6, 2024



bipyridine ligand and their use in the Ni-photoredox cross-coupling between alcohols and aryl bromides (Scheme 1A).^{12,13} In the latter transformation, continuous generation

Scheme 1. DA-Cyanoarene-Promoted Metallaphotoredox Catalytic C–O Coupling (A), Its Mechanism (B), and the Foreseen Advantage of Using a Bifunctional Photocatalyst (C)^a



^aPC = Photocatalyst; Q = Quinuclidine.

of the Ni^I complex is indispensable for both initiating and maintaining the Ni^I/Ni^{III} catalytic cycle,¹⁴ since inactive Ni^{II} species are constantly reformed by Ni^I–Ni^{III} comproportionation (Scheme 1B) and other processes.^{14,15} The Ni^{II} → Ni^I reduction step operated by PC^{•-} (Scheme 1B)^{12,15} was expected to benefit from proximity between the metal and photocatalyst (Scheme 1C), with beneficial effects on the overall reaction efficiency.¹⁶

RESULTS AND DISCUSSION

Synthesis of the Bifunctional Photocatalysts. Owing to their high catalytic activity, ready accessibility, and easy

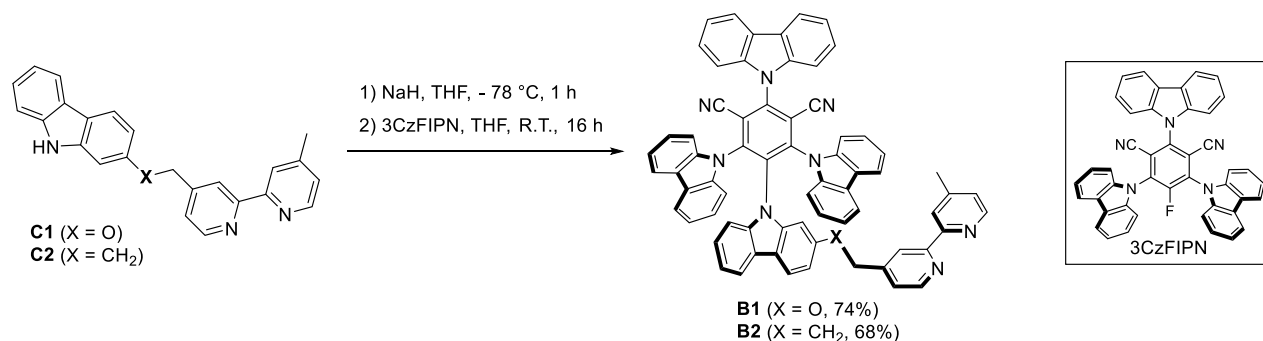
purification, donor–acceptor (DA) cyanoarenes have been successfully proposed as catalysts in photoredox organic reactions.^{12,17,18} Thus, we chose these compounds as optimal candidates for incorporation into bifunctional systems.¹⁹ As shown by Bergens and coworkers,²⁰ the different S_NAr reactivity of the *ortho/para* vs *meta* positions of perfluorocyanoarenes offers the opportunity to sequentially introduce different carbazole (Cz) residues onto the central cyanoarene core. We thus placed the functionalized carbazole moiety **C1** (synthesized from 2-hydroxycarbazole as described in Supporting Information) onto the 3CzFIPN core^{12,20} by the S_NAr reaction with the corresponding sodium salt, obtaining the bifunctional photocatalyst **B1** in good yield (Scheme 2). This system can be seen as a DA-cyanoarene conjugate possessing a bidentate ligand for binding a catalytic metal.

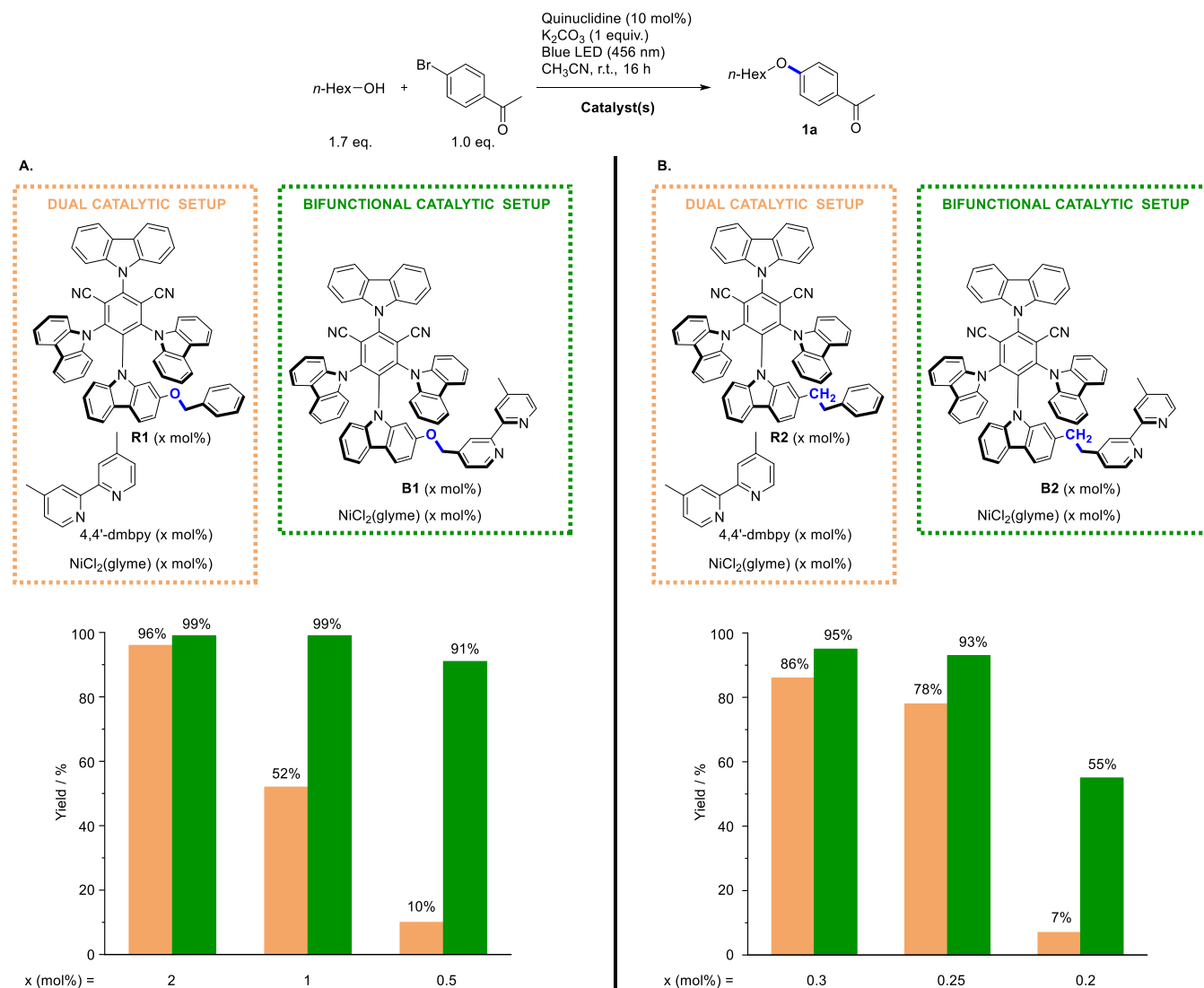
Since we expected (and later confirmed, see below) that the introduction of an oxygen substituent in one carbazole could remarkably affect the electronic and photocatalytic properties, we also prepared the bifunctional photocatalyst **B2**, possessing a CH₂ instead of an O linkage, by the same S_NAr protocol (Scheme 2). The functionalized carbazole substrate **C2** was synthesized as shown in Supporting Information. Moreover, two **B1**-analogues featuring different linkers were also prepared (compounds **B3** and **B4**, see Supporting Information) but found less active than **B1**, thus confirming the crucial importance of size and geometry of the linker to attain cooperation between the catalytic sites: the longer and relatively rigid linkers of **B3** and **B4** seemingly do not allow the intramolecular interaction between the Ni^{II}-complex and the DA-cyanoarene unit.

Assessment of Proximity Effect. To evaluate the effect of proximity, the catalytic properties of bifunctional photocatalyst **B1** (Scheme 3A) were compared with those of a dual catalytic system composed of the same, nonlinked parts in a 1:1 ratio, i.e., 4,4′-dimethyl-2,2′-dipyridyl (4,4′-dmbpy) and DA-cyanoarene **R1** (Figure 1, prepared as described in Supporting Information), bearing a benzyloxy substituent at the same position as **B1**. In the benchmark reaction of *n*-hexanol and 4-bromoacetophenone, the *in situ*-formed Ni-complexes of both catalytic systems gave good yields at relatively high catalytic loading (2 mol %). However, to our delight, when the loading was reduced to 1 and 0.5 mol %, the bifunctional system proved clearly superior to the dual, which suffered from an evident yield drop (Scheme 3A).

The higher activity of the bifunctional system [1:1 **B1**/NiCl₂(glyme)] compared to the corresponding dual catalytic system [1:1:1 **R1**/NiCl₂(glyme)/4,4′-dmbpy] was confirmed by kinetic studies on the same reaction (Figure 2). The kinetic

Scheme 2. Synthesis of the Bifunctional Photocatalysts B1 and B2



Scheme 3. Comparison between the Bifunctional Photocatalysts (B1 and B2) and the Corresponding Dual Catalytic Systems (R1 and R2) at Different Catalytic Loadings^a


^aYields were determined by ¹H NMR using 1,3,5-trimethoxybenzene as an internal standard.

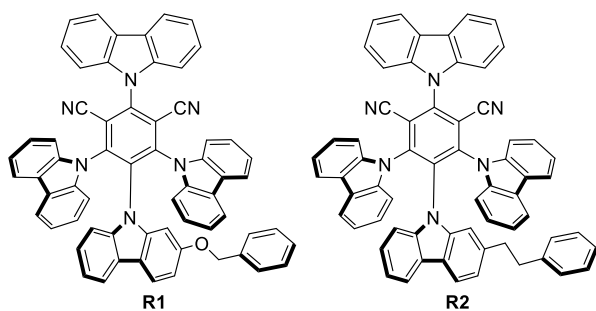


Figure 1. Reference photocatalysts employed in this study.

profiles of the reaction promoted by the bifunctional and by the dual catalyst were strikingly different: the former reached full conversion within 50 min with a downward concave profile both at 1 mol % (Figure 2A) and at 0.5 mol % catalyst loading (Figure 2B). The latter showed much slower kinetics, which, at 0.5 mol % catalyst loading (Figure 2B), did not reach full conversion even after 24 h. Notably, unlike the dual catalyst

(Figure 2A,B, orange curves), the bifunctional system displayed nearly identical kinetic profiles at 1 and 0.5 mol % loading (Figure 2A,B, green curves), consistent with the intramolecular Ni^{II} → Ni^I reduction being rate-determining in this concentration range.²¹ A possible alternative explanation of the independence of the reaction rate from [B1–Ni] might be a photon-limited regime operating at the concentrations considered.²²

The bifunctional photocatalyst **B2** was tested in the benchmark C–O coupling reaction and compared with the corresponding dual catalytic setup involving the reference DA-cyanoarene **R2** and 4,4'-dmbpy. We found that also with **B2**, a proximity effect is operating. At 0.5 mol % loading, the bifunctional setup showed a slightly steeper kinetic profile than the dual catalytic setup, which still gave full conversion (see Supporting Information). The difference between the two systems became more evident below 0.5 mol % catalyst loading, under which conditions the bifunctional system afforded higher yields than the dual one (Scheme 3B).

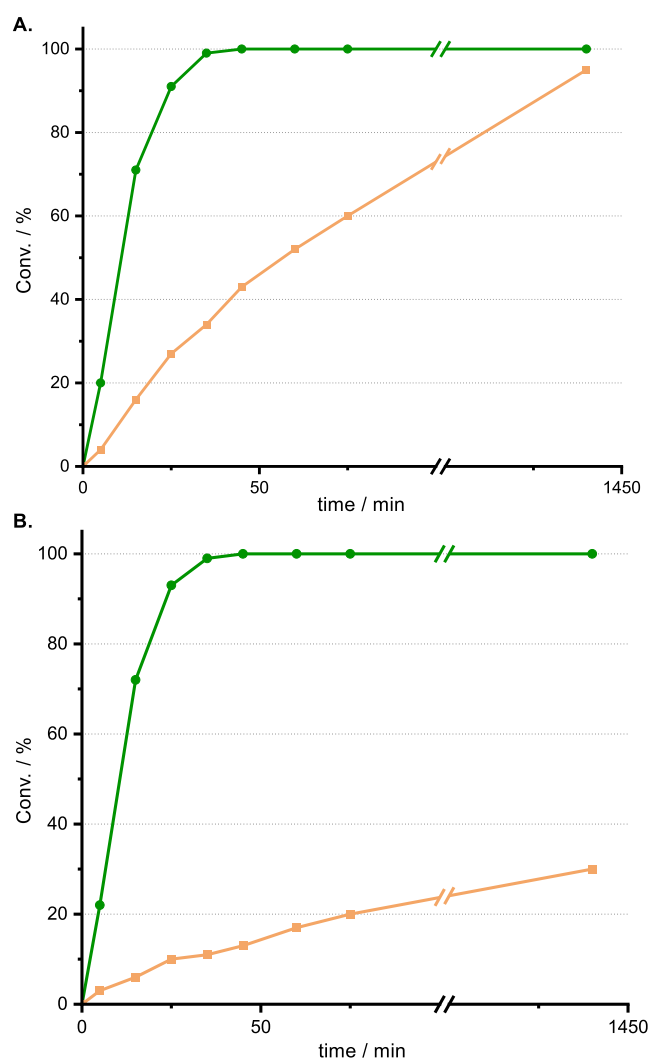


Figure 2. Kinetic profile of the reaction between *n*-hexanol and 4-bromoacetophenone with the bifunctional setup [1:1 **B1**/NiCl₂(glyme)] (●) and the dual catalytic setup [1:1:1 **R1**/NiCl₂(glyme)/4,4'-dmbpy] (■) at 1 mol % (A) and at 0.5 mol % catalyst loading (B). Conversions were determined by ¹H NMR.

Thus, bifunctionality brings higher catalytic activity for both the O-linked photocatalyst **B1** and the CH₂-linked analogue **B2**, but this is more evident in the former case. Indeed, the O-linked photocatalyst can take greater advantage from proximity because its photoactive core is intrinsically less performing due to fast nonradiative de-excitation (see below).

As a matter of fact, the bifunctional systems **B1** and **B2** allowed us to obtain similar yields in the C–O coupling of several aryl bromides with *n*-hexanol and other primary and secondary alcohols (Scheme 4), with **B1** giving slightly better results in most instances (except when poorly nucleophilic 2,2,2-trifluoroethanol was tested). Notably, the yield of the **B2**-promoted synthesis of ether **1a** was not affected by a 10× scale-up (i.e., 5 mmol instead of 0.5 mmol scale) using the same light source of the standard experiments (one Kessil light).

Photophysical Studies. The photophysical properties of the photocatalysts were investigated by UV–vis absorption and steady-state and time-resolved photoluminescence spectroscopy. The UV–vis absorption spectra of **B1**, **B2**, **R1**, **R2**, and 4CzIPN were recorded at 298 K in diluted acetonitrile (Figure

3A) and toluene solution (Figure S8). The newly synthesized photocatalysts exhibit absorption spectra very similar to the one of the parent compound 4CzIPN, characterized by strong absorption below 300 nm attributed to localized π – π^* transitions of the aromatic and carbazole units. The bipyridine moieties in **B1** and **B2** determine the higher extinction coefficient at 285 nm with respect to the other compounds. At lower energy, all of the molecules are characterized by identical broad absorption bands: a first one centered at 364 nm accounting for the n – π^* transitions and a second transition at 430 nm, ascribed to the charge transfer (CT) from the carbazolyl donor unit to the benzonitrile acceptor moiety. The steady-state photoluminescence spectra in diluted acetonitrile and toluene solutions at 298 K (Figure 3B) showed a broad and structureless emission band. Moreover, the photocatalysts **B1** and **R1**, having an electron donor oxygen bound to the carbazole, display in both solvents an emission red-shifted by about 10 nm compared to the other systems. We observed a solvatochromic effect from toluene to the more polar acetonitrile as the maximum of the low-energy absorption band blue-shifts by about 10 nm and the emission peak red-shifts by about 55 nm.

Together, the solvatochromic effect, the relevant Stokes shift in polar acetonitrile, and the absence of vibrational structure in the emission band point to the charge transfer character of the excited state, which is therefore stabilized in polar solvent.

Time-resolved experiments show a double-exponential decay character of the photoluminescence with a prompt fluorescence (PF) component in the order of nanoseconds and a delayed fluorescence (DF) component in the microsecond range for all of the compounds (see Tables 1 and S4–5). The quantum yields (Φ) of PF and DF were calculated from measurements in the presence and in the absence of oxygen. The newly synthesized photocatalysts are highly emissive in toluene, and both Φ_{PF} and Φ_{DF} are comparable to those of 4CzIPN. In acetonitrile, a decrease of the quantum yields was observed for **B2**, **R2**, and 4CzIPN, as already reported in polar solvents,²³ whereas the luminescence is suppressed in **B1** and **R1**, probably accounting for a fast nonradiative relaxation of the photoexcited species promoted by the presence of oxygen atoms.²⁴ In summary, the oxygen-sensitive fluorescence and the double-exponential decay provide evidence of the nature of TADF (thermally activated delayed fluorescence) emitters of **B1**, **B2**, **R1**, and **R2**, just as the well-known 4CzIPN.

The *in situ* formation of the **B1**–Ni complex was proved by high-resolution ESI-MS analysis of a 1:1 **B1**/[NiCl₂(glyme)] solution in acetonitrile that clearly showed the **B1**–NiCl⁺ peak as the main signal (see Supporting Information). A spectroscopic titration of a **B1** solution in DMF with the addition of NiCl₂(glyme) aliquots reveals the growth of a new absorption peak at 302 nm (see Supporting Information). The absorbance did steadily grow until a 1:1 Ni^{II}/**B1** ratio was reached, but a higher Ni^{II}/**B1** ratio did not produce further changes, thus confirming that a 1:1 complex had formed.

The photophysical properties of Ni complexes **B1**–Ni and **B2**–Ni are reported in Figure 3C and Table 1. The absorption spectra are identical to their analogous free photocatalysts except for the appearance of a shoulder at 302 nm, ascribed to the complex absorption as already observed in the spectroscopic titration. The photoluminescence of the complexes is superimposable to those of **B1** and **B2**. The complexes display TADF character; nevertheless, the PF and DF quantum yields are negligible for **B1**–Ni, as for **B1**, and are reduced for **B2**–Ni

Table 1. Photophysical and Electrochemical Properties of the Photocatalysts Involved in This Study Measured in Acetonitrile under N₂

#	Photocatalyst	$\lambda_{\text{max,em}}/\text{nm}$	Φ_{PF}^a	Φ_{DF}^b	$\tau_{\text{PF}}/\text{ns}$	$\tau_{\text{DF}}/\mu\text{s}$	$E_{0,0}/\text{eV}$	$E_{1/2}(\text{PC}^*/\text{PC}^{\bullet-})$ /V ^{c,d}	$E_{\text{onset}}(\text{PC}^{\bullet+}/\text{PC}^*)$ /V ^{c,d}	$E_{\text{onset}}(\text{PC}^{\bullet+}/\text{PC})$ /V ^e	$E_{1/2}(\text{PC}/\text{PC}^{\bullet-})$ /V ^e
1	B1	571	0.01	<0.01	30.1	1.16	2.68	1.46	-0.99	1.69	-1.22
2	B1-Ni ^e	565	0.02	<0.01	3.7	0.12	2.68	1.46	-1.12	1.56	-1.22 ^f
3	R1	572	0.01	<0.01	18.0	1.71	2.64	1.42	-1.00	1.64	-1.22
4	B2	559	0.14	0.08	20.0	2.09	2.64	1.42	-1.11	1.53	-1.22
5	B2-Ni ^e	560	0.09	<0.01	8.6	0.50	2.64	1.42	-1.10	1.54	-1.22 ^f
6	R2	560	0.14	0.10	20.2	2.07	2.63	1.41	-1.09	1.54	-1.22
7	4CzIPN	560	0.15	0.08	18.2	1.64	2.67	1.44	-1.17	1.50	-1.23

^aMeasured under air. ^bDifference between Φ measured under N₂ and under air. ^cElectrochemical potentials are referenced to the saturated calomel electrode (SCE). ^dExcited-state potentials were calculated according to the following formulas: $E(\text{PC}^*/\text{PC}^{\bullet-}) = E(\text{PC}/\text{PC}^{\bullet-}) + E_{0,0}$; $E(\text{PC}^{\bullet+}/\text{PC}^*) = E(\text{PC}^{\bullet+}/\text{PC}) - E_{0,0}$. ^eComplex generated *in situ*. ^fPotential associated with the reduction of the benzonitrile core; the reduction and oxidation potentials of Ni are omitted in this table (whole data reported in Supporting Information). The zero-zero vibrational state excitation energy $E_{0,0}$ was calculated from the intersection point between the absorption and emission spectra after the maximum intensity of emission is normalized to the absorbance at the excitation wavelength.

Overall, we found that all systems undergo a complex multielectronic oxidation at potentials over 1.99 V vs SCE (onset around 1.4 V), similarly to the behavior already observed for 4CzIPN (see Supporting Information). In contrast, a reversible monoelectronic reduction is observed, at $E_{1/2} = -1.22$ V vs SCE, for all the studied systems, and this potential is not affected by the substitution pattern on the carbazole moiety. This would imply a process mostly localized on the benzocycano core of the photocatalyst (see calculations, Table S7). A further, irreversible reduction is detected below -1.81 V vs SCE. Notably, **B1** and **B2**, featuring a bipyridine group, show a further reduction peak below -2.21 V vs SCE attributed to the monoelectronic reduction of the bipyridine system (4,4'-dmbpy was measured as reference, see Supporting Information). As expected, complexes **B1-Ni** and **B2-Ni** show a further reductive redox process at a potential slightly less negative compared to the reduction of the benzocycano core (-1.22 V vs SCE), which is compatible with the reduction process associated with the Ni^{II}/Ni^I couple ($E = -1.11$ V vs SCE), and an oxidation around 1.09 V ascribed to the Ni^{III}/Ni^{II} process (see the NiCl₂(dtbbpy) redox properties in Figure S12).^{12,25}

The Stern–Volmer quenching experiments (see Supporting Information for the graphs) confirm that the photocatalysts employed in this study (**B1-Ni**, **B2-Ni**, **R1**, and **R2**) are quenched by quinuclidine with comparable quenching constants (k_q in Table 2), despite the strong reduction of lifetimes observed in the Ni-complexes (**B1-Ni**, **B2-Ni**) with respect to the reference photocatalysts **R1** and **R2** (Table 2, entries 1, 3 vs 2, 4). This is consistent with the C–O coupling mechanism that we previously proposed (Scheme 1).^{12,15} Moreover, the improved performances of the bifunctional

Table 2. Quenching of the Photocatalysts by Quinuclidine under the Reaction Conditions^a

#	Photocatalyst	$K_{\text{SV}}/\text{mol}^{-1} \text{L}$	$\tau_{0,\text{DF}}/\mu\text{s}$	$k_q/\text{mol}^{-1} \text{L s}^{-1}$
1	B1-Ni	623	0.116	5.39×10^9
2	R1	5663	1.44	3.93×10^9
3	B2-Ni	2260	0.431	5.24×10^9
4	R2	9921	2.10	4.72×10^9
5	4CzIPN	10625	1.67	6.36×10^9

^aData collected from Stern–Volmer plots of delayed lifetimes (excitation at 375 nm) in Ar-degassed acetonitrile.

photocatalysts with respect to the dual systems at decreased loading suggest that an intramolecular step involving Ni^{II} → Ni^I reduction could operate after the photocatalyst is quenched by quinuclidine.

CONCLUSIONS

In this paper, we have described a bifunctional catalytic approach involving conjugation of an organic photocatalyst to a bpy ligand that can bind transition metals. Using the metallaphotoredox Ni-catalyzed C–O cross-coupling as a model reaction, we have demonstrated that proximity between the two catalytic moieties (i.e., the metal complex and DA-cyanoarene) is beneficial for catalytic activity, which is higher than the one displayed by the corresponding dual catalytic system. The bifunctional photocatalysts have been shown to be able to promote the coupling of several primary and secondary alcohols to aryl bromides at low catalytic loading. This work represents one of the first examples of bifunctional DA-cyanoarene,^{12,15} and—to the best of our knowledge—the first in which these TADF-emitters are linked to a bidentate ligand. We believe that the proof-of-concept provided by this work may serve as a basis to further implement the “bifunctional approach” in photocatalysis, exploring other types of metal, reactivity, and catalyst design.

ASSOCIATED CONTENT

Data Availability Statement

The data underlying this study are available in the published article and in its Supporting Information.

Supporting Information

The Supporting Information is available free of charge at <https://pubs.acs.org/doi/10.1021/acscatal.4c05893>.

General procedures, experimental details, characterization data, NMR spectra, and fluorescence quenching experiments (PDF)

AUTHOR INFORMATION

Corresponding Authors

Marta Penconi – Istituto di Scienze e Tecnologie Chimiche “Giulio Natta” (SCITEC) del Consiglio Nazionale delle Ricerche (CNR), Milano 20138, Italy; SmartMatLab Center, Milano 20133, Italy; orcid.org/0000-0001-7459-7354; Email: marta.penconi@cnr.it

Luca Pignataro – Università degli Studi di Milano,
Dipartimento di Chimica, Milano 20133, Italy;
orcid.org/0000-0002-7200-9720;
Email: luca.pignataro@unimi.it

Authors

Luigi Dolcini – Università degli Studi di Milano,
Dipartimento di Chimica, Milano 20133, Italy;
orcid.org/0000-0001-9455-9785

Andrea Solida – Università degli Studi di Milano,
Dipartimento di Chimica, Milano 20133, Italy

Daniele Lavelli – Università degli Studi di Milano,
Dipartimento di Chimica, Milano 20133, Italy;
orcid.org/0000-0003-4847-7409

Andrés Mauricio Hidalgo-Núñez – Università degli Studi di
Milano, Dipartimento di Chimica, Milano 20133, Italy;
orcid.org/0009-0007-7884-3525

Tommaso Gandini – Università degli Studi di Milano,
Dipartimento di Chimica, Milano 20133, Italy; Present
Address: Università degli Studi di Milano, Dipartimento
di Scienze Farmaceutiche, via Venezian 21 20133 Milano,
Italy; orcid.org/0000-0002-3682-914X

Matthieu Fornara – Università degli Studi di Milano,
Dipartimento di Chimica, Milano 20133, Italy

Alessandro Colella – Università degli Studi di Milano,
Dipartimento di Chimica, Milano 20133, Italy

Alberto Bossi – Istituto di Scienze e Tecnologie Chimiche
“Giulio Natta” (SCITEC) del Consiglio Nazionale delle
Ricerche (CNR), Milano 20138, Italy; SmartMatLab Center,
Milano 20133, Italy; orcid.org/0000-0001-9252-6218

Daniele Fiorito – Dipartimento di Chimica, Materiali e
Ingegneria Chimica “Giulio Natta”, Politecnico di Milano,
Milano 20133, Italy; orcid.org/0000-0002-6950-7446

Cesare Gennari – Università degli Studi di Milano,
Dipartimento di Chimica, Milano 20133, Italy;
orcid.org/0000-0002-7635-4900

Alberto Dal Corso – Università degli Studi di Milano,
Dipartimento di Chimica, Milano 20133, Italy;
orcid.org/0000-0003-4437-8307

Complete contact information is available at:
<https://pubs.acs.org/10.1021/acscatal.4c05893>

Author Contributions

The manuscript was written through contributions of all authors. All authors have given approval to the final version of the manuscript.

Funding

We thank the European Commission (European Union's Horizon Europe research and innovation program, Marie Skłodowska-Curie Grant Agreement no. 101119574 “Next-Base”) for a Ph.D. fellowship (to A.M.H.N.) and financial support. M.P. and A.B. gratefully acknowledge Regione Lombardia and Fondazione Cariplo for funding the SmartMatLab Centre project.

Notes

The authors declare no competing financial interest.

ACKNOWLEDGMENTS

Mass spectrometry analyses were performed at the Mass Spectrometry facility of the Unitech COSPECT at the University of Milan (Italy).

REFERENCES

- (1) (a) Liu, X.; Lin, L.; Feng, X. Amide-based bifunctional organocatalysts in asymmetric reactions, *Chem. Commun.*, **2009**, 6145–6158. (b) Serdyuk, O. V.; Heckel, C. M.; Tsoogoeva, S. B. Bifunctional primary amine-thioureas in asymmetric organocatalysis. *Org. Biomol. Chem.* **2013**, *11*, 7051–7071. (c) Chauhan, P.; Mahajan, S.; Kaya, U.; Hack, D.; Enders, D. Bifunctional Amine-Squaramides: Powerful Hydrogen-Bonding Organocatalysts for Asymmetric Domino/Cascade Reactions. *Adv. Synth. Catal.* **2015**, *357*, 253–281. (d) Zhang, Z.-W.; Liu, S.-W.; Huang, H.-P.; Xie, Y.-H.; Huang, R.-C.; Deng, Y.-Q.; Lin, N. Dehydroabietane-type bifunctional organocatalysts in asymmetric synthesis: recent progress. *RSC Adv.* **2023**, *13*, 31047–31058.
- (2) (a) Sandee, A. J.; Reek, J. N. H. Bidentate ligands by supramolecular chemistry—the future for catalysis?, *Dalton Trans.*, **2006**, 3385–3391. (b) Carboni, S.; Gennari, C.; Pignataro, L.; Piarulli, U. Supramolecular ligand-ligand and ligand-substrate interactions for highly selective transition metal catalysis. *Dalton Trans.* **2011**, *40*, 4355–4373. (c) Morris, R. H. Exploiting Metal–Ligand Bifunctional Reactions in the Design of Iron Asymmetric Hydrogenation Catalysts. *Acc. Chem. Res.* **2015**, *48*, 1494–1502. (d) Dixon, D. J. Bifunctional catalysis. *Beilstein J. Org. Chem.* **2016**, *12*, 1079–1080. (e) Pignataro, L.; Gennari, C. Riding the Wave of Monodentate Ligand Revival: From the A/B Concept to Noncovalent Interactions. *Chem. Rec.* **2016**, *16*, 2544–2560. (f) Morris, R. H. Iron Group Hydrides in Noyori Bifunctional Catalysis. *Chem. Rec.* **2016**, *16* (6), 2644–2658. (g) Ugwu, D. I.; Conradie, J. Bidentate ligands in self-assembly: Synthesis, structure and applications. *J. Mol. Struct.* **2023**, *1293*, 136275.
- (3) (a) Rolka, A. B.; König, B. Bifunctional organic photocatalysts for enantioselective visible-light-mediated photocatalysis. *Nat. Synth.* **2023**, *2*, 913–925. (b) Shen, J.-H.; Shi, M.; Wei, Y. Synergistic Visible Light Photocatalysis with Organocatalysis. *Chem.-Eur. J.* **2023**, *29*, No. e202301157.
- (4) Roy, S.; Paul, H.; Chatterjee, I. Light-Mediated Aminocatalysis: The Dual-Catalytic Ability Enabling New Enantioselective Route. *Eur. J. Org. Chem.* **2022**, No. 25, No. e202200446.
- (5) (a) Rigotti, T.; Casado-Sánchez, A.; Cabrera, S.; Pérez-Ruiz, R.; Liras, M.; de la Peña O'Shea, V. A.; Alemán, J. A Bifunctional Photoaminocatalyst for the Alkylation of Aldehydes: Design, Analysis, and Mechanistic Studies. *ACS Catal.* **2018**, *8*, 5928–5940. (b) Gualandi, A.; Calogero, F.; Martinelli, A.; Quintavalla, A.; Marchini, M.; Ceroni, P.; Lombardo, M.; Cozzi, P. G. A supramolecular bifunctional iridium photoaminocatalyst for the enantioselective alkylation of aldehydes. *Dalton Trans.* **2020**, *49*, 14497–14505.
- (6) (a) Alonso, R.; Bach, T. A Chiral Thioxanthone as an Organocatalyst for Enantioselective [2 + 2] Photocycloaddition Reactions Induced by Visible Light. *Angew. Chem. Int. Ed.* **2014**, *53*, 4368–4371. (b) Frost, J. R.; Huber, S. M.; Breitenlechner, S.; Bannwarth, C.; Bach, T. Enantiotopos-Selective C-H Oxygenation Catalyzed by a Supramolecular Ruthenium Complex. *Angew. Chem. Int. Ed.* **2015**, *54*, 691–695. (c) Böhm, A.; Bach, T. Synthesis of Supramolecular Iridium Catalysts and Their Use in Enantioselective Visible-Light-Induced Reactions. *Synlett* **2016**, *27*, 1056–1060. (d) Tröster, A.; Alonso, R.; Bauer, A.; Bach, T. Enantioselective Intermolecular [2 + 2] Photocycloaddition Reactions of 2(1H)-Quinolones Induced by Visible Light Irradiation. *J. Am. Chem. Soc.* **2016**, *138*, 7808–7811. (e) Hölzl-Hobmeier, A.; Bauer, A.; Silva, A. V.; Huber, S. M.; Bannwarth, C.; Bach, T. Catalytic deracemization of chiral allenes by sensitized excitation with visible light. *Nature* **2018**, *564*, 240–243. (f) Tröster, A.; Bauer, A.; Jandl, C.; Bach, T. Enantioselective Visible-Light-Mediated Formation of 3-Cyclopropylquinolones by Triplet-Sensitized Deracemization. *Angew. Chem. Int. Ed.* **2019**, *58*, 3538–3541. (g) Li, X.; Jandl, C.; Bach, T. Visible-Light-Mediated Enantioselective Photoreactions of 3-Alkylquinolones with 4-O-Tethered Alkenes and Allenes. *Org. Lett.* **2020**, *22*, 3618–3622. (h) Plaza, M.; Jandl, C.; Bach, T. Photochemical Deracemization of Allenes and Subsequent Chirality Transfer. *Angew. Chem. Int. Ed.* **2020**, *59*, 12785–12788. (i) Li, X.; Kutta, R. J.; Jandl, C.; Bauer, A.;

- Nuernberger, P.; Bach, T. Photochemically Induced Ring Opening of Spirocyclopropyl Oxindoles: Evidence for a Triplet 1,3-Diradical Intermediate and Deracemization by a Chiral Sensitizer. *Angew. Chem. Int. Ed.* **2020**, *59*, 21640–21647. (j) Plaza, M.; Großkopf, J.; Breitenlechner, S.; Bannwarth, C.; Bach, T. Photochemical Deracemization of Primary Allene Amides by Triplet Energy Transfer: A Combined Synthetic and Theoretical Study. *J. Am. Chem. Soc.* **2021**, *143*, 11209–11217. (k) Li, X.; Großkopf, J.; Jandl, C.; Bach, T. Enantioselective, Visible Light Mediated Aza Paternò–Büchi Reactions of Quinoxalinones. *Angew. Chem. Int. Ed.* **2021**, *60*, 2684–2688. (l) Kratz, T.; Steinbach, P.; Breitenlechner, S.; Storch, G.; Bannwarth, C.; Bach, T. Photochemical Deracemization of Chiral Alkenes via Triplet Energy Transfer. *J. Am. Chem. Soc.* **2022**, *144*, 10133–10138.
- (7) Mayr, F.; Mohr, L.-M.; Rodriguez, E.; Bach, T. Synthesis of Chiral Thiourea-Thioxanthone Hybrids. *Synthesis* **2017**, *49*, 5238–5250.
- (8) (a) Pecho, F.; Zou, Y.-Q.; Gramüller, J.; Mori, T.; Huber, S. M.; Bauer, A.; Gschwind, R. M.; Bach, T. A Thioxanthone Sensitizer with a Chiral Phosphoric Acid Binding Site: Properties and Applications in Visible Light-Mediated Cycloadditions. *Chem.-Eur. J.* **2020**, *26*, 5190–5194. (b) Lyu, J.; Claraz, A.; Vitale, M. R.; Allain, C.; Masson, G. Preparation of Chiral Photosensitive Organocatalysts and Their Application for the Enantioselective Synthesis of 1,2-Diamines. *J. Org. Chem.* **2020**, *85*, 12843–12855. (c) Pecho, F.; Sempere, Y.; Gramüller, J.; Hörmann, F. M.; Gschwind, R. M.; Bach, T. Enantioselective [2 + 2] Photocycloaddition via Iminium Ions: Catalysis by a Sensitizing Chiral Brønsted Acid. *J. Am. Chem. Soc.* **2021**, *143*, 9350–9354. (d) Lyu, J.; Leone, M.; Claraz, A.; Allain, C.; Neuville, L.; Masson, G. Syntheses of new chiral chimeric photoorganocatalysts. *RSC Adv.* **2021**, *11*, 36663–36669. (e) Takagi, R.; Tanimoto, T. Enantioselective [2 + 2] photocycloaddition of quinolone using a C₁-symmetric chiral phosphoric acid as a visible-light photocatalyst. *Org. Biomol. Chem.* **2022**, *20*, 3940–3947. (f) Rolka, A. B.; Archipowa, N.; Kutta, R. J.; König, B.; Toste, F. D. Hybrid Catalysts for Enantioselective Photo-Phosphoric Acid Catalysis. *J. Org. Chem.* **2023**, *88*, 6509–6522.
- (9) (a) Tang, X.-F.; Feng, S.-H.; Wang, Y.-K.; Yang, F.; Zheng, Z.-H.; Zhao, J.-N.; Wu, Y.-F.; Yin, H.; Liu, G.-Z.; Meng, Q.-W. Bifunctional metal-free photo-organocatalysts for enantioselective aerobic oxidation of β -dicarbonyl compounds. *Tetrahedron.* **2018**, *74*, 3624–3633. (b) Tang, X.-F.; Zhao, J.-N.; Wu, Y.-F.; Zheng, Z.-H.; Feng, S.-H.; Yu, Z.-Y.; Liu, G.-Z.; Meng, Q.-W. Enantioselective photooxygenation of β -dicarbonyl compounds in batch and flow photomicroreactors. *Org. Biomol. Chem.* **2019**, *17*, 7938–7942. (c) Tang, X.-F.; Zhao, J.-N.; Wu, Y.-F.; Feng, S.-H.; Yang, F.; Yu, Z.-Y.; Meng, Q.-W. Visible-Light-Driven Enantioselective Aerobic Oxidation of β -Dicarbonyl Compounds Catalyzed by Cinchona-Derived Phase Transfer Catalysts in Batch and Semi-Flow. *Adv. Synth. Catal.* **2019**, *361*, 5245–5252.
- (10) (a) Ding, W.; Lu, L.-Q.; Zhou, Q.-Q.; Wei, Y.; Chen, J.-R.; Xiao, W.-J. Bifunctional Photocatalysts for Enantioselective Aerobic Oxidation of β -Ketoesters. *J. Am. Chem. Soc.* **2017**, *139*, 63–66. (b) Yin, H.; Wang, C.-J.; Zhao, Y.-G.; He, Z.-Y.; Chu, M.-M.; Wang, Y.-F.; Xu, D.-Q. Asymmetric bis(oxazoline)-Ni(II) catalyzed α -hydroxylation of cyclic β -keto esters under visible light. *Org. Biomol. Chem.* **2021**, *19*, 6588–6592.
- (11) Lee, J.; Song, W. J. Photocatalytic C–O Coupling Enzymes That Operate via Intramolecular Electron Transfer. *J. Am. Chem. Soc.* **2023**, *145*, 5211–5221.
- (12) Gandini, T.; Dolcini, L.; Di Leo, L.; Fornara, M.; Bossi, A.; Penconi, M.; Dal Corso, A.; Gennari, C.; Pignataro, L. Metallophotoredox C–O and C–N Cross-Coupling Using Donor-Acceptor Cyanoarene Photocatalysts. *ChemCatchem* **2022**, *14* (23), No. e202200990.
- (13) Terrett, J. A.; Cuthbertson, J. D.; Shurtleff, V. W.; MacMillan, D. W. C. Switching on elusive organometallic mechanisms with photoredox catalysis. *Nature* **2015**, *524*, 330–334.
- (14) For examples of Ni^{II}→Ni^I reduction by oxidative quenching of the photoexcited species, see: (a) Na, H.; Mirica, L. M. Deciphering the mechanism of the Ni-photocatalyzed C–O cross-coupling reaction using a tridentate pyridinophane ligand. *Nat. Commun.* **2022**, *13* (1), 1313. (b) Bao, L.-Y.; Gao, R.-W.; Wang, S.; Li, R.-H.; Zhu, B.; Su, Z.-M.; Guan, W. Theoretical study of Ni^I–Ni^{III} cycle mediated by heterogeneous zinc in C–N cross-coupling reaction. *Phys. Chem. Chem. Phys.* **2022**, *24*, 7617–7623. (c) Chrisman, C. H.; Kudisch, M.; Puffer, K. O.; Stewart, T. K.; Lamb, Y. M. L.; Lim, C.-H.; Escobar, R.; Thordarson, P.; Johannes, J. W.; Miyake, G. M. Halide Noninnocence and Direct Photoreduction of Ni(II) Enables Coupling of Aryl Chlorides in Dual Catalytic, Carbon–Heteroatom Bond-Forming Reactions. *J. Am. Chem. Soc.* **2023**, *145*, 12293–12304.
- (15) (a) For C–O coupling, see: Sun, R.; Qin, Y.; Rucolo, S.; Schnedermann, C.; Costentin, C.; Nocera, D. G. Elucidation of a Redox-Mediated Reaction Cycle for Nickel-Catalyzed Cross-Coupling. *J. Am. Chem. Soc.* **2019**, *141*, 89–93. (b) For C–N coupling, see: Till, N. A.; Tian, L.; Dong, Z.; Scholes, G. D.; MacMillan, D. W. C. Mechanistic Analysis of Metallaphotoredox C–N Coupling: Photocatalysis Initiates and Perpetuates Ni(I)/Ni(III) Coupling Activity. *J. Am. Chem. Soc.* **2020**, *142*, 15830–15841.
- (16) Generation of the Ni^I catalytic species from photoactive Ni^{II} complexes in the absence of a photocatalyst has also been reported. See: (a) Shields, B. J.; Kudisch, B.; Scholes, G. D.; Doyle, A. G. Long-Lived Charge-Transfer States of Nickel(II) Aryl Halide Complexes Facilitate Bimolecular Photoinduced Electron Transfer. *J. Am. Chem. Soc.* **2018**, *140*, 3035–3039. (b) Ting, S. I.; Garakharaghi, S.; Taliaferro, C. M.; Shields, B. J.; Scholes, G. D.; Castellano, F. N.; Doyle, A. G. ³d-d Excited States of Ni(II) Complexes Relevant to Photoredox Catalysis: Spectroscopic Identification and Mechanistic Implications. *J. Am. Chem. Soc.* **2020**, *142*, 5800–5810. (c) Yang, L.; Lu, H.-H.; Lai, C.-H.; Li, G.; Zhang, W.; Cao, R.; Liu, F.; Wang, C.; Xiao, J.; Xue, D. Light-Promoted Nickel Catalysis: Etherification of Aryl Electrophiles with Alcohols Catalyzed by a Ni^{II}-Aryl Complex. *Angew. Chem. Int. Ed.* **2020**, *59*, 12714–12719. (d) Cagan, D. A.; Strocio, G. D.; Cusumano, A. Q.; Hadt, R. G. Multireference Description of Nickel–Aryl Homolytic Bond Dissociation Processes in Photoredox Catalysis. *J. Phys. Chem. A* **2020**, *124*, 9915–9922. (e) Cagan, D. A.; Bím, D.; Silva, B.; Kazmierczak, N. P.; McNicholas, B. J.; Hadt, R. G. Elucidating the Mechanism of Excited-State Bond Homolysis in Nickel–Bipyridine Photoredox Catalysts. *J. Am. Chem. Soc.* **2022**, *144*, 6516–6531. (f) Cavedon, C.; Gisbertz, S.; Reischauer, S.; Vogl, S.; Sperlich, E.; Burke, J. H.; Wallick, R. F.; Schrottke, S.; Hsu, W.-H.; Anghileri, L.; et al. Intraligand Charge Transfer Enables Visible-Light-Mediated Nickel-Catalyzed Cross-Coupling Reactions. *Angew. Chem. Int. Ed.* **2022**, *61* (46), No. e202211433.
- (17) Dolcini, L.; Gandini, T.; Castiglioni, R.; Bossi, A.; Penconi, M.; Dal Corso, A.; Gennari, C.; Pignataro, L. Visible Light-Promoted β -Functionalization of Carbonyl Compounds in the Presence of Organic Dyes. *J. Org. Chem.* **2023**, *88*, 14283–14291.
- (18) (a) Luo, J.; Zhang, J. Donor–Acceptor Fluorophores for Visible-Light-Promoted Organic Synthesis: Photoredox/Ni Dual Catalytic C(sp³)–C(sp²) Cross-Coupling. *ACS Catal.* **2016**, *6*, 873–877. (b) Speckmeier, E.; Fischer, T. G.; Zeitler, K. A Toolbox Approach To Construct Broadly Applicable Metal-Free Catalysts for Photoredox Chemistry: Deliberate Tuning of Redox Potentials and Importance of Halogens in Donor–Acceptor Cyanoarenes. *J. Am. Chem. Soc.* **2018**, *140*, 15353–15365.
- (19) For examples of use of DA cyanoarenes in bifunctional catalysis, see: (a) Rolka, A. B.; Archipowa, N.; Kutta, R. J.; König, B.; Toste, F. D. Hybrid Catalysts for Enantioselective Photo-Phosphoric Acid Catalysis. *J. Org. Chem.* **2023**, *88* (10), 6509–6522. (b) Chao, D.; Zhao, M. A supramolecular assembly bearing an organic TADF chromophore: synthesis, characterization and light-driven cooperative acceptorless dehydrogenation of secondary amines. *Dalton Trans.* **2019**, *48* (16), 5444–5449.
- (20) Rasu, L.; Amiri, M.; Bergens, S. H. Carbazole–Cyanobenzene Dyes Electrografted to Carbon or Indium-Doped Tin Oxide Supports

for Visible Light-Driven Photoanodes and Olefin Isomerizations. *ACS Appl. Mater. Interfaces* **2021**, *13*, 17745–17752.

(21) With catalyst loadings lower than 0.2 mol% the yields substantially dropped.

(22) For studies considering photon-limited vs photon unlimited regime in Ni-photoredox cross coupling, see: (a) Malik, J. A.; Madani, A.; Pieber, B.; Seeberger, P. H. Evidence for Photocatalyst Involvement in Oxidative Additions of Nickel-Catalyzed Carboxylate O-Arylations. *J. Am. Chem. Soc.* **2020**, *142*, 11042–11049. (b) Madani, A.; Pieber, B. In situ Reaction Monitoring in Photocatalytic Organic Synthesis. *ChemCatChem* **2023**, *15* (7), No. e202201583.

(23) Ishimatsu, R.; Matsunami, S.; Shizu, K.; Adachi, C.; Nakano, K.; Imato, T. Solvent Effect on Thermally Activated Delayed Fluorescence by 1,2,3,5-Tetrakis(carbazol-9-yl)-4,6-dicyanobenzene. *J. Phys. Chem. A* **2013**, *117*, 5607–5612.

(24) For an example of substituent effect on the PC's de-excitation pathway, see: Sayre, H.; Ripberger, H. H.; Odella, E.; Zieleniewska, A.; Heredia, D. A.; Rumbles, G.; Scholes, G. D.; Moore, T. A.; Moore, A. L.; Knowles, R. R. PCET-Based Ligand Limits Charge Recombination with an Ir(III) Photoredox Catalyst. *J. Am. Chem. Soc.* **2021**, *143*, 13034–13043.

(25) Oderinde, M. S.; Frenette, M.; Robbins, D. W.; Aquila, B.; Johannes, J. W. Photoredox Mediated Nickel Catalyzed Cross-Coupling of Thiols With Aryl and Heteroaryl Iodides via Thiyl Radicals. *J. Am. Chem. Soc.* **2016**, *138*, 1760–1763.



CAS BIOFINDER DISCOVERY PLATFORM™

**PRECISION DATA
FOR FASTER
DRUG
DISCOVERY**

CAS BioFinder helps you identify
targets, biomarkers, and pathways

Unlock insights

CAS
A division of the
American Chemical Society